arXiv:cond-mat/9905166v1 [cond-mat.str-el] 12 May 1999

Kinematics of electrons near a Van Hove singularity

J. González [1], F. Guinea [2] and M. A. H. Vozmediano [3]
[1] *Instituto de Estructura de la Materia. Consejo Superior de Investigaciones Científicas. Serrano 123, 28006 Madrid. Spain.*
[2] *Instituto de Ciencia de Materiales. Consejo Superior de Investigaciones Científicas. Cantoblanco. 28049 Madrid. Spain.*
[3] *Departamento de Matemáticas. Universidad Carlos III. Avenida de la Universidad 30. Leganés. 28913 Madrid. Spain.*
(February 1, 2008)

A two dimensional electronic system, where the Fermi surface is close to a Van Hove singularity, shows a variety of weak coupling instabilities, and it is a convenient model to study the interplay between antiferromagnetism and anisotropic superconductivity. We present a detailed analysis of the kinematics of the electron scattering in this model. The similitudes, and differences, between a standard Renormalization Group approach and previous work based on parquet summations of $\log^2$ divergences are analyzed, with emphasis on the underlying physical processes. General properties of the phase diagram are discussed.

75.10.Jm, 75.10.Lp, 75.30.Ds.

Since the discovery of high-T_c superconductivity, the study of interacting electrons in two dimensions has been a topic of wide interest. A great variety of numerical and analytical techniques have been developed. Progress has been relatively slow, and there is little consensus on the phase diagram of even the simplest models. In the following, we revisit one of the most extensively studied models, interacting electrons in a single band whose Fermi surface lies close to a Van Hove singularity. Interest in this model arose rapidly after the two dimensional character of the electron bands in the cuprates was established [1–5]. Since then, a number of different analytical approaches have been tried [6–10]. Its interest increased when photoemission experiments showed the existence of almost dispersionless regions near the Fermi surface [11], leading to renewed efforts to understand the mechanism for superconductivity using this feature.

A few facts seem to be well established about the model: i) It is unstable, even at weak coupling, making it similar to the one dimensional Luttinger liquids and ii) Among the possible instabilities, antiferromagnetism and d-wave superconductivity seem to be the most likely candidates in a wide range of parameters, although ferromagnetism can also exist [12,13]. These features (apart from ferromagnetism) where already discussed in the early papers on the model. It is thus surprising the little progress made in the intervening period.

The purpose of the present paper is to disentangle the various factors which complicate the study of the model, and to study the interplay and coexistence between superconductivity and antiferromagnetism. As discussed in detail below, the apparent similarities with one dimensional systems have lead to approximations which miss important features of the kinematics of electrons in two dimensions. This neglect, in turn, gives rise to the main difficulty in the study of the model, the fact that the perturbative divergences mentioned before seem to go like the square of the logarithm of the cutoff. This feature, never found in a renormalizable field theory in the usual sense, has been dealt with by parquet summation techniques, using the analogy with one dimensional systems. While these approximations have their own merits, they cannot be considered a proper implementation of a Renormalization Group procedure. In the following, we extend previous results, and present a detailed analysis of the renormalization of interactions in this model, using the by now standard approach presented in [14–16]. The present work shows that the Van Hove singularity problem can be treated by techniques which are easily extended to generic two dimensional problems, allowing us to extrapolate the phase diagram to different ranges of parameters and fillings.

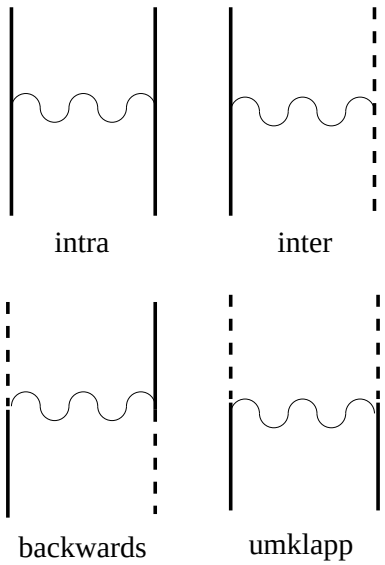

FIG. 1. Bare couplings. Full and dashed lines stand for propagators at the two inequivalent saddle points.

We focus on the weak coupling instabilities of the model. As mentioned earlier, a perturbation analysis shows that, unlike models with isotropic Fermi surfaces, the RG flow of the electron-electron interactions is not trivial. We consider only the electronic states lying near the two inequivalent saddle points of a square lattice. Following preceding analyses, we classify the couplings into

four groups, shown in Fig. 1, denoted as intrasingularity, intersingularity, backwards and Umklapp scattering. In addition to this, the conservation of total momentum, and the requirement that the scattered electrons lie close to the Fermi surface induce new constraints. The pair of outgoing momenta is uniquely determined by the pair of incoming momenta, except when they add up to zero [14,16]. This allows us to define the Cooper pair channel in this latter instance, besides the forward and exchange channels, that open up when the momentum transfer to any of the outgoing particles vanishes (modulo (π,π) in the present model).

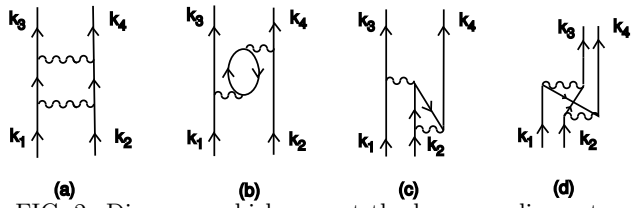

FIG. 2. Diagrams which correct the bare couplings at one loop.

The lowest order corrections to the bare couplings are shown in Fig. 2. In a conventional Fermi liquid, only the diagram (a) in Fig. 2 depends logarithmically on the cutoff, leading to the BCS instability. In the present case all diagrams show logarithmic dependences, if the momentum of the excitations which are integrated over is close to zero. The ladder diagram (a) in Fig. 2 shows a $\log^2(\Lambda)$ dependence, while the others behave as $\log(\Lambda)$. We are not considering the possibility of perfect nesting, when the Fermi surfaces at the two singularities are parallel [17].

We first discuss the diagrams (b), (c) and (d) in Fig. 2. The restriction on the intermediate momenta implies that the divergences appear when $\vec{k}_1 \approx \vec{k}_3$. Thus, diagrams (b) and (c) give non trivial corrections in the forward channel, and diagram (d) modifies the exchange channel. Note however that, when all spins are parallel, the forward and exchange channels can only be distinguished by the momentum transfer involved, as they lead to the same final state. Physical observables depend only on the difference between them, like the direct and $2k_F$ scattering between electrons with parallel spin in one dimension. In the following, we make use of this fact and redefine the parallel forward channel as this combination. In this way, the exchange channel only has antiparallel couplings. Furthermore, the forward channel is only renormalized by couplings in the forward channel. The same applies to the exchange and Cooper pair channels.

With the mentioned redefinition of the forward parallel couplings, the net effect of the renormalization is given by diagram (b), which tends to screen the bare interaction. The RG equations in the forward channel are:

$$
\begin{aligned}
\frac{\partial u_{F\mathrm{intra}\parallel}}{\partial l} &= -\frac{1}{4\pi^2 t} c \left(u^2_{F\mathrm{intra}\perp} + u^2_{F\mathrm{inter}\perp} + \right. \\
&\quad \left. + \, u^2_{F\mathrm{intra}\parallel} + u^2_{F\mathrm{inter}\parallel} \right) \\
\frac{\partial u_{F\mathrm{intra}\perp}}{\partial l} &= -\frac{1}{2\pi^2 t} c \left(u_{F\mathrm{intra}\parallel} u_{F\mathrm{intra}\perp} + u_{F\mathrm{inter}\parallel} u_{F\mathrm{inter}\perp} \right) \\
\frac{\partial u_{F\mathrm{inter}\parallel}}{\partial l} &= -\frac{1}{2\pi^2 t} c \left(u_{F\mathrm{intra}\perp} u_{F\mathrm{inter}\perp} + u_{F\mathrm{intra}\parallel} u_{F\mathrm{inter}\parallel} \right) \\
\frac{\partial u_{F\mathrm{inter}\perp}}{\partial l} &= -\frac{1}{2\pi^2 t} c \left(u_{F\mathrm{intra}\parallel} u_{F\mathrm{inter}\perp} + u_{F\mathrm{intra}\perp} u_{F\mathrm{inter}\parallel} \right) \\
\frac{\partial u_{F\mathrm{back}\parallel}}{\partial l} &= -\frac{1}{4\pi^2 t} c' \left(u^2_{F\mathrm{back}\perp} + u^2_{F\mathrm{umk}\perp} + \right. \\
&\quad \left. + \, u^2_{F\mathrm{back}\parallel} + u^2_{F\mathrm{umk}\parallel} \right) \\
\frac{\partial u_{F\mathrm{back}\perp}}{\partial l} &= -\frac{1}{2\pi^2 t} c' \left(u_{F\mathrm{back}\parallel} u_{F\mathrm{back}\perp} + u_{F\mathrm{umk}\parallel} u_{F\mathrm{umk}\perp} \right) \\
\frac{\partial u_{F\mathrm{umk}\parallel}}{\partial l} &= -\frac{1}{2\pi^2 t} c' \left(u_{F\mathrm{back}\perp} u_{F\mathrm{umk}\perp} + u_{F\mathrm{back}\parallel} u_{F\mathrm{umk}\parallel} \right) \\
\frac{\partial u_{F\mathrm{umk}\perp}}{\partial l} &= -\frac{1}{2\pi^2 t} c' \left(u_{F\mathrm{back}\parallel} u_{F\mathrm{umk}\perp} + u_{F\mathrm{back}\perp} u_{F\mathrm{umk}\parallel} \right)
\end{aligned}
\tag{1}
$$

where c, c' are the prefactors of the polarizabilities at zero and $\mathbf{Q} = (\pi,\pi)$ momentum transfer. A formally equivalent equation is obtained for the couplings in the exchange channel, except that, in this case, the signs in the r. h. s. of Eq. (1) are positive, and repulsive couplings increase upon scaling. The equations in (1) can be further simplified. For instance, we can add and substract the upper four equations, to obtain:

$$
\begin{aligned}
\frac{\partial \left(u_{F\mathrm{intra}\parallel} \pm u_{F\mathrm{inter}\parallel} \right)}{\partial l} &= -\frac{1}{4\pi^2 t} c \left[\left(u_{F\mathrm{intra}\perp} \pm u_{F\mathrm{inter}\perp} \right)^2 + \right. \\
&\quad \left. + \, \left(u_{F\mathrm{intra}\parallel} \pm u_{F\mathrm{inter}\parallel} \right)^2 \right] \\
\frac{\partial \left(u_{F\mathrm{intra}\perp} \pm u_{F\mathrm{inter}\perp} \right)}{\partial l} &= -\frac{1}{4\pi^2 t} c \left(u_{F\mathrm{intra}\parallel} \pm u_{F\mathrm{inter}\parallel} \right) \times \\
&\quad \left(u_{F\mathrm{intra}\perp} \pm u_{F\mathrm{inter}\perp} \right)
\end{aligned}
\tag{2}
$$

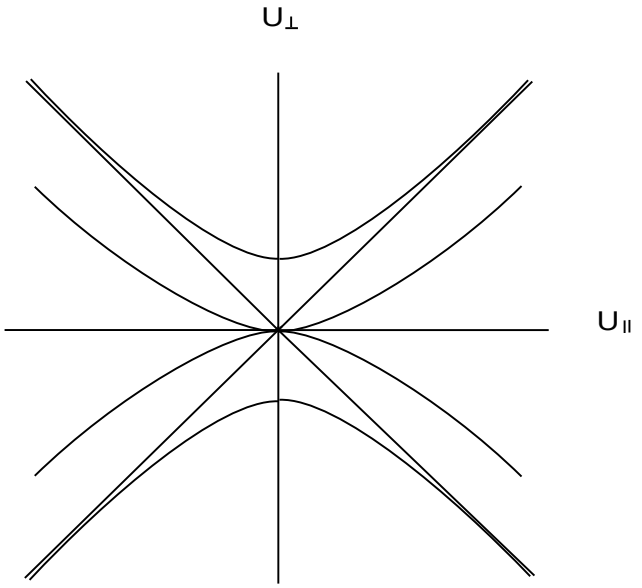

FIG. 3. Generic flow of the couplings. The flow direction is towards the left in the forward channel, for the combination of couplings in Eq. (2). A similar flow diagram can be drawn for the Cooper pair channel, with the replacement of $u_{\parallel}, u_{\perp}$ by the Cooper pair couplings $u_{C\mathrm{intra}\perp}, u_{C\mathrm{umk}\perp}$.

These equations can be integrated analytically. The main features of the flow are depicted in Fig. 3. The flow for the forward channel is towards negative values of the abscissas, the opposite as for the exchange channel. The hamiltonian flows towards different fixed points for different initial conditions, defining different universality classes. When the initial couplings are spin independent [3,5,10], the flow starts at the diagonal. The couplings in the forward channel vanish in the infrared. If the bare hamiltonian is the Hubbard model in its usual form, the initial parallel couplings are zero. Then, the couplings must flow towards a strong coupling regime. If only the forward and exchange channels are considered, the leading instability is towards a broken symmetry state with antiferro- or ferromagnetic order, depending on whether c' or c is larger. It is easy to show that the (attractive) divergent flow of the parallel couplings in the forward channel matches the repulsive flow of the antiparallel couplings in the exchange channel. The two channels renormalize the parallel and transverse spin-spin correlations, respectively, so that the flow maintains the original SU(2) symmetry of the microscopic model. In the following, we consider the modifications to this picture induced by the inclusion of the Cooper channel, which has to be considered independently.

The main source of difficulties, the $\log^2$ divergences in the perturbation expansion, is found in the Cooper channel. A number of previous works have dealt with them by scaling the couplings as function of $\log^2(\Lambda)$, instead of the more standard $\log(\Lambda)$. Let us consider in some detail the implications of this procedure. In a renormalizable theory in the usual sense, an effective hamiltonian can be defined at each scale, Λ, with dimensionless interactions, $\{\tilde{u}_i\}$, that depend on Λ. The elegance of the method resides in the fact that there is no explicit dependence on Λ elsewhere. The most general equation for the flow of the couplings is:

$$\Lambda \frac{\partial \tilde{u}_i}{\partial \Lambda} = f\left(\{\tilde{u}_j\}, \frac{\Lambda}{\Delta}\right) \tag{3}$$

where the functions f are dimensionless and Δ stands for additional low energy scales. The statement that the model is renormalizable implies that the limit $\Delta/\Lambda \to 0$ can be safely taken. On the other hand, a scaling with $\log^2$ implies that the r. h. s. of Eq. (3) is of the type:

$$f\left(\{\tilde{u}_j\}, \frac{\Lambda}{\Delta}\right) = \tilde{f}(\{\tilde{u}_j\}) \log\left(\frac{\Lambda}{\Delta}\right) \tag{4}$$

The dependence on the low energy scales represented by Δ cannot be avoided. A scaling in terms of $\log^2$ is not equivalent to a conventional RG calculation, as it ignores the low energy scales present in the flow equations. It resembles more a parquet summation of leading divergences. In one dimension, where only logarithmic divergences appear, both approaches are equivalent. This is not the case in the present problem. It can be shown [9] that a $\log^2$ divergence, when inserted into a self energy diagram, leads to further $\log^2$ divergences in the one electron propagator. The usual wavefunction renormalization cannot take care of this divergence, signalling again the existence of hidden scales and/or new, non local interactions.

In order to avoid the $\log^2$ divergences in the Cooper channel, we move the chemical potential slightly away from the singularity. It is easy to show that the divergence in the Cooper channel becomes $\log(\Lambda/\omega)\log(\Lambda/\mu)$, where μ is the chemical potential. If $\mu \ll \Lambda$, the other channels are unaffected. The factor $\log(\Lambda/\mu)$ is simply the density of states at the Fermi level, which, in principle, can also be scale dependent. A full treatment of this term requires the analysis of the flow of the chemical potential itself.

We will assume that the system is in contact with an external reservoir which fixes the physical, fully renormalized chemical potential. The effective chemical potential which must be inserted into the low energy hamiltonian at a scale Λ is renormalized by a Hartree diagram [14]. In the present case, this diagram has a logarithmic singularity, besides the usual linear dependence on Λ dictated by dimensional considerations [14,9]. As a result, one finds for the dimensionless chemical potential, $\tilde{\mu} = \mu/\Lambda$:

$$\frac{\partial \tilde{\mu}}{\partial \log(\Lambda)} = \tilde{\mu} - (\tilde{u}_{F\mathrm{intra}} + \tilde{u}_{F\mathrm{inter}}) \log\left(\frac{1}{1-\tilde{\mu}}\right) \tag{5}$$

where a summation over parallel and perpendicular spin orientations is assumed, and the couplings have been written in a dimensionless form. This equation has a stable fixed point, $\tilde{\mu}^*$. This fixed point is attained if $\tilde{\mu} > 0$, that is, if the chemical potential lies above the singularity. The existence of this fixed point is crucial in simplifying the treatment of the scaling in the Cooper channel. For sufficiently small initial couplings or at sufficiently low energies, we can replace the $\log(\Lambda/\mu)$ in the scaling of the couplings in the Cooper channel by the constant $\log(1/\tilde{\mu}^*)$. Note that the previous analysis does not contradict the conservation of the number of electrons implied in Luttinger's theorem, as we have chosen to work at fixed external chemical potential. We find that this is the natural choice in the problem at hand. The restriction of the study to small patches near the saddle points is justified as these regions give rise to the main divergences in perturbation theory. However, the remaining sections of the Fermi surface are, at least, a reservoir of electrons, always in contact with the system studied here.

The previous discussion shows that one of the two $\log(\Lambda)$ factors which appear in the Cooper channel should

not be included in the RG equations, provided that the chemical potential is shifted slightly away from the singularity. The resulting equations are analogous to those in Eq. (1), except that the coefficients include a constant equal to $\log(1/\tilde{\mu}^*)$ at the beginning of the scaling. Note, finally, that the existence of a finite chemical potential implies that the flow in Eqs. (1) ceases to be valid at $\omega \sim \mu$. On the other hand, the couplings reach a strong coupling regime at scales $E_c \sim \Lambda e^{-1/u_0}$ where u_0 stands for the initial dimensionless couplings. Hence, the phase diagram, which is determined by the couplings which reach first the strong coupling limit, should be independent of μ, provided that $\mu \ll E_c$.

We now analyze the phase diagram by identifying the couplings which diverge at the highest scale. A simple inspection shows that ferromagnetism prevails when $c > c'$, associated with the divergences in $u_{F\mathrm{intra}\parallel}, u_{F\mathrm{intra}\perp}, u_{F\mathrm{inter}\parallel}$ and $u_{F\mathrm{inter}\perp}$. When $c < c'$ the leading divergences are either in the set $\{u_{F\mathrm{back}\parallel}, u_{F\mathrm{back}\perp}, u_{F\mathrm{umk}\parallel}, u_{F\mathrm{umk}\perp}\}$ or in the couplings for the Cooper channel $u_{C\mathrm{intra}\perp}$ and $u_{C\mathrm{umk}\perp}$. The first set gives rise to antiferromagnetism, while the second pair leads to d-wave superconductivity, even if the initial couplings are repulsive, provided that $u_{C\mathrm{umk}\perp} > u_{C\mathrm{intra}\perp} > 0$ as shown in Fig. 3. In the Hubbard model, these couplings are initially equal. Finite corrections, not considered here, influence differently $u_{C\mathrm{umk}\perp}$ and $u_{C\mathrm{intra}\perp}$, leading to the conditions for d-wave superconductivity. These finite corrections are those considered by Kohn and Luttinger in their pioneering work on anisotropic superconductivity from repulsive interactions [18].

Thus, the phases which arise in a weak coupling treatment of the Hubbard model near a Van Hove singularity are ferromagnetism antiferromagnetism and d-wave superconductivity. The competition between antiferromagnetism and superconductivity depends on the value of c' and $\log(\mu^*)$. As both types of couplings diverge, the transition between the two is discontinuous (the phase diagram in the strong coupling limit to which the system flows should be well described within a mean field approximation with the appropiate couplings [19]). Finally, the charge compressibility depends on the density of states at the Fermi level divided by one plus the sum of the parallel and antiparallel couplings in the intrasingularity forward channel. As discussed earlier, parallel couplings flow towards divergent negative values, while antiparallel couplings are divergent and positive. The sum tends to zero. Thus, the compressibility approaches the density of states, which, by definition, is large. We find no evidence of a vanishing compressibility [10]. On the other hand, we cannot rule out that the cancellation found here does not exist when the Fermi level is sufficiently far from the singularity, leading to an infinite compressibility and phase separation [20].

In conclusion, we have analyzed in detail the kinematics of electrons near a two dimensional Van Hove singularity. While the model has been studied extensively, the classification of the different allowed channels has never been presented. This framework, which makes connexion with standard applications of the Renormalization Group program to two and three dimensional electronic systems [14], clarifies the different physical processes involved, and the main features of the phase diagram. The results can differ substantially from those obtained by summing, in an uncontrolled way, $\log^2(\Lambda)$ divergences. Finally, it can be easily extended to address other types of anisotropic Fermi surfaces [21,22].

[1] J. Labbé and J. Bok, *Europhys. Lett.* **3** (1987) 1225.

[2] J. Friedel, *J. Phys.* (Paris) **48** (1987) 1787; **49** (1988) 1435.

[3] H. J. Schulz, *Europhys. Lett.* **4**, 609 (1987).

[4] J. E. Dzyaloshinskii, *Pis'ma Zh. Eksp. Teor. Fiz.* **46**, 97 (1987) [*JETP Lett.* **46**, 118 (1987)]. I. E. Dzyaloshinskii and V. M. Yakovenko, Sov. Phys. JETP **67**, 844 (1988).

[5] P. Lederer, G. Montambaux and D. Poilblanc, J. Physique **48**, 1613 (1987).

[6] R. S. Markiewicz and B. G. Giessen, *Physica* (Amsterdam) **160C** (1989) 497. R. S. Markiewicz, *J. Phys. Condens. Matter* **2** (1990) 665.

[7] D. M. Newns *et al.*, *Phys. Rev. Lett.* **69**, 1264 (1992).

[8] L. B. Ioffe and A. J. Millis, *Phys. Rev.* **B 54** (1996) 3645.

[9] J. González, F. Guinea and M. A. H. Vozmediano, *Europhys. Lett.* **34**, 711 (1996). J. González, F. Guinea and M. A. H. Vozmediano, *Nucl. Phys.* **B 485** (1997) 694.

[10] N. Furukawa, T. M. Rice and M. Salmhofer, *Phys. Rev. Lett.* **81**, 3195 (1998).

[11] Z.-X. Shen *et al.*, *Science* **267**, 343 (1995).

[12] S. Sorella, R. Hlubina and F. Guinea, *Phys. Rev. Lett.* **78** (1997) 1343.

[13] J. V. Alvarez, J. González, F. Guinea and M. A. H. Vozmediano, *J. Phys. Soc. Jpn.* **67**, 1868 (1998).

[14] R. Shankar, Rev. Mod. Phys. **66**, 129 (1994).

[15] J. Polchinski in *Proceedings of the 1992 TASI in Elementary Particle Physics*, J. Harvey and J. Polchinski eds., World Scientific (Singapore) 1992. A. C. Hewson, Adv. Phys. **43**, 143 (1994).

[16] W. Metzner, C. Castellani and C. di Castro, Adv. Phys. **47**, 3 (1998).

[17] If we use a tight binding scheme to describe the electron bands, the case of parallel Fermi lines corresponds to $t' = 0$, in the usual language. All available evidence suggests that the model is antiferromagnetic with long range order at zero temperature.

[18] W. Kohn and J. M. Luttinger, *Phys. Rev. Lett.* **15**, 524 (1965).

[19] M. Murakami and H. Fukuyama, J. Phys. Soc. Jpn. **67**, 2784 (1998).

[20] M. Murakami, `Possible Ordered States in the 2D Hubbard Model` preprint (cond-mat/9904213).

[21] J. González, F. Guinea and M. A. H. Vozmediano, *Phys. Rev. Lett.* **79**, 3514 (1997).

[22] D. Zanchi and H. J.

Schulz, *Phys. Rev.* **B54**, 9509 (1996). D. Zanchi and H. J. Schulz, `Weakly correlated electrons on a square lattice: a renormalization group theory`, preprint (cond-mat/9812303).